Process Design Kits for Co-Designing Broadband Integrated Photonics and Silicon CMOS in Electronic-Photonic VLSI Circuits

Georgios Kyriazidis[†,1], John Davis[1], Jui-Hung Chang[1,2], Hana Warner[1], Normann Lippok[1,3], Chih-Lung Lin[2], Benjamin J. Vakoc[3], Marko Loncar[1], and Gage Hills[1]

[1]Harvard School of Engineering and Applied Sciences (SEAS), [2]National Cheng Kung University, [3]Wellman Ctr. for Photomedicine

gkyriazidis@g.harvard.edu

***Abstract*—Electronic-Photonic Integrated Circuits (EPICs) are evolving rapidly for high performance communication, computation, imaging, and more. However, optimizing performance for EPICs is challenging due to the separate tools used for designing photonic and electronic components, while the interconnect between the two often limits the overall EPIC performance. Thus, co-designing, simulating, and verifying electronics, photonics, and their interconnect together, in a unified design environment is essential. To address this, we present Process Design Kits (PDKs) for co-designing electronics, photonics, and interconnect parasitics using industry-standard VLSI design flows. Key characteristics of our PDKs include: (1) SPICE-compatible compact models for photonic devices, enabling circuit simulations for ICs comprising both electronic and photonic devices as well as their interconnection. (2) Techniques to account for broad optical spectrums and non-linear interactions between wavelengths, e.g., non-linear optical processes in semiconductor optical amplifiers and second harmonic generation. (3) Physical design and verification, with parameterized cells for layouts, and tools for automatic Design Rule Check (DRC) and Layout vs. Schematic (LVS). We demonstrate the effectiveness of our PDKs with detailed physical designs and simulations for applications including: (a) high-speed optical datalinks leveraging resonators to implement wavelength-division multiplexing (WDM); and (b) high-bandwidth computation kernels for matrix multiplication in the optical domain.**

***Index Terms*—Electro-Photonic Process Design Kit, PDK**

I. Introduction

EPICs offer significant performance benefits across a wide range of applications, including: high-speed communication [1], clock-tree distribution for chiplet-based computing systems [2], optical computing [3], LiDAR [4], interfaces to quantum systems [5], metamaterial-based flat optics [6], and medical imaging [7], [8]. Recent advances in *on-chip integrated photonics* allow for the fabrication of numerous photonic devices using standard VLSI process flows, which leverage decades of semiconductor fabrication developments with minimal changes [9]. For example, the Thin-Film Lithium Niobate (TFLN) platform is an emerging technology for high-performance integrated photonics [10], and a promising alternative to Silicon Photonics, due to its advantageous material properties such as high electro-optic coefficient, for efficient and high-speed modulation, and second-order non-linearities, employed for Second-Harmonic Generation (SHG) [11]. Furthermore, advancements in *heterogeneous integration* can be used to physically connect photonic circuit elements (e.g., optical amplifiers), electronic circuit elements (e.g., transceivers), and circuit elements for electronic-photonic interfaces (e.g., lasers, photodetectors), with various advanced packaging techniques for both the photonic [12]) and electronic [13] domains, such as photonic wire-bonding and face-to-face bonding.

However, the physical design complications arising in VLSI *design* due to heterogeneous integration [14], also affect EPICs that utilize similar VLSI *fabrication* processes. Providing support and leveraging the infrastructure of industry-standard VLSI design flows, including CAD tools and models for simulation, physical design, and optimization, is essential for the success of EPICs. While this infrastructure is actively being developed (e.g., CAD tool support for design and analysis of photonic circuits [15]), outstanding complications remain.

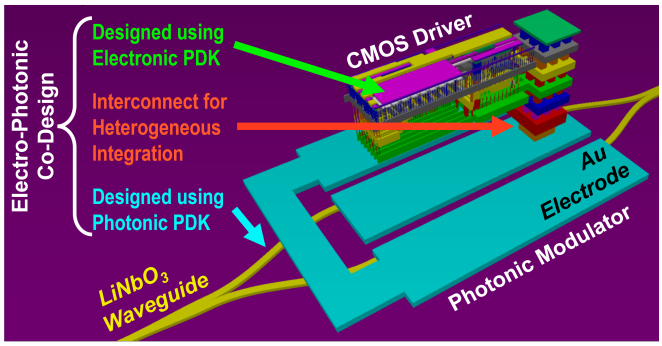

Fig. 1. Example EPIC. The full circuit comprises high-speed electronic drivers (silicon CMOS) heterogeneously integrated (face-to-face) with an electro-optical modulator (Mach-Zehnder Modulator) in TFLN.

A key issue, we address in this paper, is *electronic-photonic co-design* - crucial for maximizing EPIC performance - which faces *design challenges* from both technical and practical perspectives. Some of the challenges include:

- **Challenge 1 – Tools Integration:** Different CAD *tools* are used for simulations of electronics (e.g., Cadence Spectre, Synopsys HSPICE) and photonics (e.g., Ansys Lumerical), due to the fundamentally different physics behind the electrical and optical domains, with non-streamlined information transfer procedures. Importantly, many EPICs rely on *feedback* between electronic and photonic circuit elements, and their performance is limited by their interactions. Designing such systems are challenging without a unified design environment that understands *both* domains.
- **Challenge 2 – PDK Compatibility:** Electrical ICs (EICs) and Photonic ICs (PICs) currently rely on separate PDKs, developed without integration in mind, which is particularly limiting for heterogeneously integrated EPICs (e.g., EICs communicating through a photonic interposer). These PDKs, typically provided by different foundries, hinder the co-design and integration process. Furthermore, they lack support for physical verification, including automated DRC and LVS, for the EIC-PIC interconnections.

- **Challenge 3 – Compact Modelling:** Transient simulations in the photonic domain, operating at hundreds of THz, are computationally intensive. When combined with GHz-range electronic simulations, the computational and storage demands escalate, as each electronic periods involves simulating thousands of photonic periods. Additionally, there are multiple options to represent light (e.g, intensity, E-field, M-field), each with varying trade-offs between accuracy and resource usage. This parallels the complexities in the electronic domain, where specialized software (e.g., Synopsys Sentaurus) captures the unterline device physics of a transistor and encodes a tuned transfer function, based on lumped voltage and current, to a compact model.

In this paper, we present EPIC PDKs that overcome these challenges and enable co-design of electronic and photonic circuits in a singular design environment, leveraging industry-standard VLSI tools and development methodologies. Our EPIC PDKs, described in the following sections, are summarized in the reference design of Figure 1 and our key contributions are:

1) **Techniques for simulating *broadband electronic-photonic circuits*** using conventional circuit simulators (e.g., Cadence Spectre). Our "broadband simulations" account for multiple wavelengths of optical signals *simultaneously*, in stark contrast to simulations that analyze many wavelengths *independently*. This enables circuit simulators to model *interactions* between different optical wavelengths, essential for *non-linear* photonic devices, like Semiconductor Optical Amplifiers (SOAs) which exhibits non-linear effects such as optical power saturation, and Second Harmonic Generation (SHG) devices whose output power at a specific wavelength (λ_1) depends non-linearly to the input power at multiple wavelengths (including λ_1 and $\lambda_2 = 0.5\lambda_1$). Our broadband simulation techniques are described in Section II-A.
2) **Publicly-available EPIC PDKs**, comprising: (a) compact device models that implement our broadband simulation techniques for a wide range of electronic-photonic devices, including Micro-Ring Resonators (MRRs), Mach-Zehnder Interferometers (MZIs), SOAs, lasers, photodetectors, grating couplers and more (Section II-B); (b) integration of standard silicon CMOS PDKs, photonic PDKs, and interconnect techniques for heterogeneous integration (Section II-C); and (c) support for layout design and physical verification (DRC, LVS) using widely-used CAD tools (Cadence Virtuoso and Siemens Calibre). For example, our reference EPIC PDKs enable designs using face-to-face bonding that connects a 180 nm silicon CMOS Electronic IC (EIC) with a Thin-Film Lithium Niobate (TFLN, $LiNbO_3$) Photonic IC (PIC). Our compact models are written in Verilog-A - compatible with standard circuit simulators - and can be instantiated in the same circuit netlists with electronic devices. They are parameterized across a wide range of electrical and optical parameters, and they are calibrated to electro-magnetic simulation results and experimentally measured data.
3) **Reference physical designs and simulations accross multiple applications** to demonstrate the effectiveness of our EPIC PDKs and the critical role of electro-optical co-optimization. For instance, in [8], co-optimization boosts the modulator iso-power bandwidth by $\times 100$ compared to the optical-only optimization applied in [7]. The reference applications (Section III) include: (a) high-speed optical datalinks leveraging Mach-Zender Modulators (MZMs), Micro-Ring Resonators (MRRs) for Wavelength-Division Multiplexing (WDM); and (b) high-bandwidth computation kernels for matrix multiplication in the optical domain programmable through an electrical interface.

II. EPIC PDKs

Figure 2 illustrates how our EPIC PDKs fit into a co-design framework for Electronic-Photonic Integrated Circuits. We combine innovations in photonic PDKs (described in this paper) that enable industry-standard CAD tools (e.g., Cadence Virtuoso and Cadence Spectre) to simulate and optimize silicon CMOS circuits and integrated photonic circuits in a *unified design environment*. SPICE-compatible compact models, calibrated with electromagnetic (E&M) simulation data and experimental measurements of fabricated PICs (Figure 2). are incorporated into EPIC PDKs for the design, optimization, and tape-out of electronic-photonic integrated circuits.

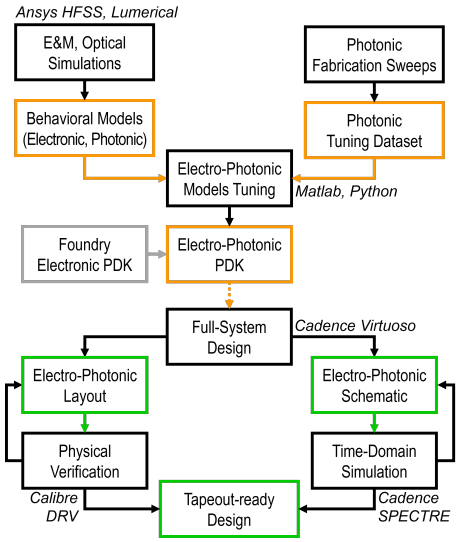

Fig. 2. Electro-photonic Design Framework. The results from electro-magnetic simulations and fabrication sweeps are combined into highly-tuned physics compact models. Parametrizable physical layouts are added on top of the SPICE models to form a Electro-Photonic PDK that can be combined with Electronic PDK from commercial foundries. The user performs a full-system design with both layout and schematic views, verifying the correct operation through physical verification (DRC, LVS) and time-domain simulations.

A. Broadband Photonic Simulations

For broadband simulations, we first explain how photonic signals are encoded to allow computationally-efficient simulation of photonic device behavior. Next, we detail how our compact device models align with this encoding of photonic information and interface with standard circuit simulators.

Finally, we discuss how our compact models fascilitate the co-design of electronic and photonic circuit elements.

Photonic signals can be characterized by various properties, including (but not limited to): optical power vs. electromagnetic field strength, time domain vs. frequency domain representation, optical mode (e.g., single mode waveguide vs. multimode waveguide), and their frequency/wavelength spectrum. The electrical specialization of standard circuit simulations makes mapping of optical information (e.g., E-field, intensity) to electrical properties (e.g. voltage, current) non-trivial due to differing physical behavior. We select an encoding for photonic signals that widens the generality of the models and enables computationally-efficient broadband electronic-photonic circuit simulations:

- **Optical signals are represented in the *frequency domain* rather than the *time domain***. Typical frequencies of interest for photonic circuits are on the order of hundreds of THz (e.g., $\nu = 300$ THz for an optical wavelength of $\lambda = 1.0$ μm), making transient simulations at this resolution computationally intensive. Instead, the spectrum of interest can be compressed by using a discrete set of frequencies across it with minimal accuracy loss, as demonstrated in Section II-B. For instance, a WDM electro-optical transceiver that transmits data on eight optical frequencies (channels) centered at $\nu = 193.55$ THz ($\lambda \approx 1.550$ μm) with a free-spectral range of $FSR = 100$ GHz can sample the frequency spectrum within $\nu \in [193.1, 194.0]$ THz at a 5 GHz spacing, as demonstrated in Section III. This approach avoids unnecessary computations for unsupported optical frequencies and is visual described in Figure 3.
- **At each physical location along the center of an optical waveguide, the photonic signal at that point is represented by a vector of *phasors***. Each phasor corresponding to a singular combination of the afforementioned discrete optical *frequency* and optical *mode*. Note that, if the waveguide is designed to support only a single mode, then only one phasor per frequency is needed, as in all the examples described in this paper. Phasors store both the amplitude and relative phase of the electric field (E-field) of photonic signals, which is crucial for simulators to understand signals interactions. For example, two single-mode inputs into a y-combiner will constructively interfere if they are in phase, or will partially couple into a higher-order mode if they are out of phase with each other. Thus, encoding photonic signals by optical power alone would be insufficient.
- **Phasors should be processed by their *real* and *imaginary* components** (i.e., their projections onto the real and imaginary axises), rather than by their amplitude and phase. As described later in this section, we express these real and imaginary components as *voltages*; although they are not actually voltages. This representation allows us to "trick" standard circuit simulators into processing optical domain signals (a technique also used by image sensor PDKs, where ideal an voltage source represents the incident optical power on a photodiode). While the real/imaginary and amplitude/phase representations are mathematically equivalent, some electrical circuit simulators struggle with the equivalence of 0 and 2π radians, which can hinder convergence algorithms and would limit the generality of our solution.

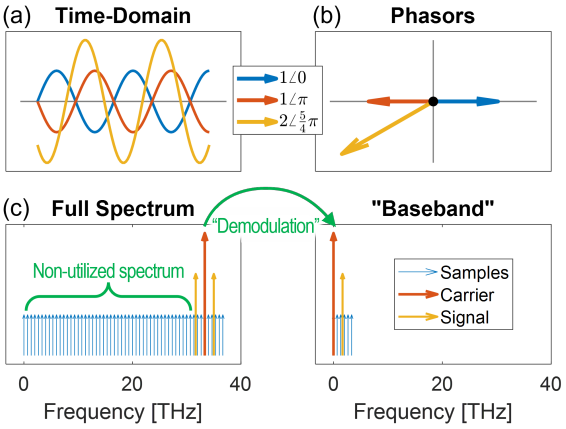

Fig. 3. Encoding of photonic signals. (a) Time-domain representation (electric field vs. time) of three optical signals with identical frequency but different amplitudes and phases. (b) Corresponding E-field phasor representations, which represents the envelope of the optical signals for computational efficiency. (c) Each sampled frequency is represented by a phasor, demodulated around a carrier frequency. Information in the "non-utilized spectrum", which includes unsupported by the waveguide frequencies, can be excluded while retaining simulation accuracy. This enables the design of compact device models that manipulates these phasors, using transfer functions with optical inputs/outputs expressed in baseband, while preserving the essential physics of photonic devices across a broad spectrum of wavelengths.

We now describe how the phasor representation is integerated in compact models for processing using circuit simulators. For instance, Figure 4 illustrates a schematic testbench for our MZI compact model. For N sampled wavelengths and a single-mode waveguide, there are $2N$ optical inputs - two for the real and imaginary parts of each E-field phasor - and $2N$ optical outputs. These $2N$ inputs are parameterized as an array of nets, where the "voltage" on each net corresponds to the magnitude of the real part or imaginary part of the E-field phasor. The Verilog-A compact model can compute the $2N$ optical outputs using information from all $2N$ optical inputs *simultaneously*; this is especially important for non-linear devices where the output at *each* wavelength may depend on the input at *multiple* wavelengths, such as the SOA described in the next (Section II-B).

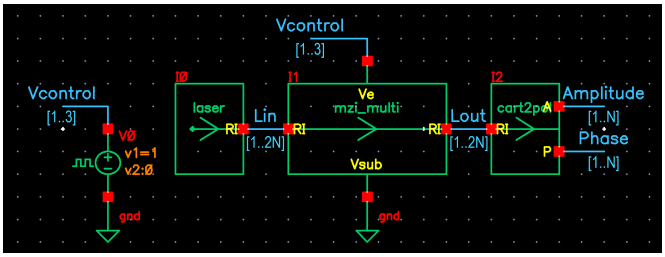

Fig. 4. Schematic testbench for our MZI compact model. An array of ideal voltage sources drives the "Lin" input array ("Light Input") to the MZI compact model, which interprets voltage as the magnitude of the real/imaginary components of the E-field phasor. The "cart2pol" symbol converts real/imaginary components of "Lout" ("Light Output") into phase/amplitude, as an option for viewing output waveforms.

Compact Model		Description
Utility (Non-physical)	laser	Outputs an array of E-field phasors across a broad spectrum of wavelengths with a parameterizable spectrum
	resonator	Models an ideal spectral transfer function (sinusoidal, exponential, ring-like)
	soa	Semiconductor Optical Amplifier, amplifies input considering gain saturation, spectral broadening & spontaneous emission
	cart2pol	Utility for waveform plots: converts between cartesian coordinates (real/imaginary) & polar coordinates (phase/amplitude)
Devices (Physical)	waveguide	Propagation & loss of E-field phasors, accounts for temperature-dependent phase shift due to electrical heaters
	yjunction	Functions either as a y-splitter (*N* inputs to *2N* outputs) or y-combiner (*2N* inputs to *N* outputs), including extrinsic loss
	directional_coupler	Maps *2N* inputs to *2N* outputs with wavelength-dependent splitting (dependent on physical parameters for coupling)
	grating_coupler	Accounts for transfer function of E-field through an optical grating coupler, depending on its bandwidth and loss
	eo	Electro-Optical phase shifter, similar to a waveguide with the addition of electrically-controlled phase shift
	mzi	Mach-Zehnder Interferometer with parameterizable number of branches (B), implemented using 'yjunction' and 'eo' models
	mrr	Micro-Ring Resonator, implemented using 'directional_coupler' and 'waveguide' models
	photodiode	Converts *N* optical inputs into electrical current between 2 electrical ports (depends on the photodiode spectral response)

Fig. 5. Compact models included as part of our EPIC PDK. Extensive details will be provided as part of the public release [**?**]. All compact models are implemented using plain text, so we expect users should be able to easily adjust parameters and compact models based on their specific application targets.

Figure 5 lists our compact models implementing the broadband simulation techniques. Each model integrates with Cadence Virtuoso via OpenAccess objects, including: schematic symbol, performance estimation scripts before simulation - e.g., V_π of MZIs, Free Spectral Range (FSR) of MRRs - circuit simulation testbench, parameters tuned on devices of in-house TFLN Platform, parameterizable cell layout, and DRC/LVS rules (for physical verification using Siemens Calibre).

Our Verilog-A models also define wavelength-dependent behavior. Algorithm 1 outlines how we calculate the effective refractive index (n_{eff}) as a function of wavelength, using a first-order Taylor series expansion; while supporting higher-order models for higher accuracy. We derive the complex effective refractive index (n_{eff}), the loss (a) and the input-output phase difference ($\Delta\phi$), the group (g) and phase (ϕ) velocity (v) of a wave packet, and the delay (Δt) over a specified path length (PL) from parameters extracted from electro-magnetic simulations (e.g., Ansys Lumerical).

Algorithm 1 Characteristics of i-th wavelength

$$\Delta\lambda = \lambda_i - \lambda_{center}$$
$$n_i = Re\{n_{eff}\} = n_{eff@center} + n_{slope} * \Delta\lambda$$
$$\kappa_i = Im\{n_{eff}\} = \kappa_{eff@center} + \kappa_{slope} * \Delta\lambda$$
$$a = 20 * log(e^{2\pi/\lambda_{center} * \kappa_i * PL}) \ [dB]$$
$$\Delta\phi = 2\pi * n_i * PL/\lambda_i$$
$$v_\phi = c_0/n_i \quad ; v_g = c_0/(n_i - \lambda_i * n_{slope})$$
$$\Delta t_\phi = PL/v_\phi \ ; \ \Delta t_g = PL/v_g$$

Additionally, we leverage standard electrical inputs in Verilog-A to allow interactions between the electrical and optical domains. For example, each MZI electrode in Figure 4 has a corresponding electrical input that can be driven using standard electrical circuit elements (e.g., high-speed drive circuitry) and is used to compute (a) the electric field that modulates the optical outputs; and (b) the RC network seen by the electrical driver. This enables the *time-dependent* response of devices influenced by the transitioning of the electrical input signals. Details of our MZI compact model are shown in Figure 6 (physical layout and parameters) and Algorithm 2 (compact model algorithm) in the following section.

Finally, we cross-verify the operation of the devices. For example, in Figure 7, we simulate a challenging-to-model device, a Micro-Ring Resonator (MRR), using the extracted performance metrics from electro-magnetic simulations (e.g., coupling coefficients, inter-ring losses from Ansys Lumerical) and observe the minimal discrepancies in the spectral response between the finite-element solution and the compact model.

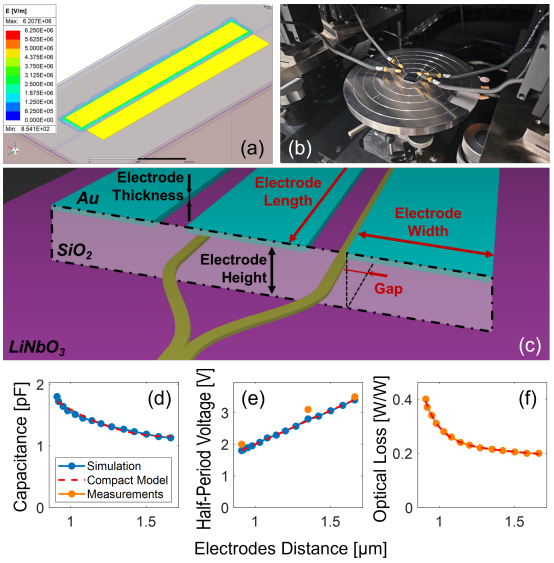

Fig. 6. Physical Characteristics of Photonic Devices. Through (a) electro-magnetic simulations and (b) experimental measurements on fabricated chips, (c) the physical dimensions of structure are related to the performance metrics of the devices. In this example, (d) the electrode capacitance, (e) the half-period voltage and (f) the optical loss of an MZI are related to the distance of the electrodes from the waveguide; $distance = \sqrt{height^2 + gap^2}$.

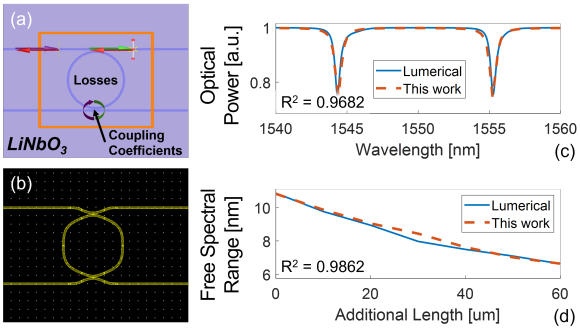

Fig. 7. Verification of MRR. An equivalent model was simulated in (a) Lumerical FDTD and (b our PDK). The 2D electro-magnetic simulations, running for 17 $minutes$, yielded: a coupling coefficient (τ) of 0.99, an inter-ring optical path length (l_{inter}) of 219.3μm and attenuation (α_{inter}) of 1.1dB. The spectral responses are compared in (c) nominal geometry, and both result in a $-2.4dB$ Extinction Rate (ER) and 10.8nm Free Spectral Range (FSR). Also, by keeping the extracted parameters and varying the inter-ring path length, (d) we validate the predictive behavior of our compact model, with each simulation completed in 1 $minute$ ($\times 17$ $speedup$).

B. Compact Models for Electronic-Photonic Devices

Here, we describe a set of compact models implementing the broadband simulation techniques discussed previosuly, enabling the design of EPICs for a wide range of applications (examples provided in Section III).

Our models are calibrated for PICs fabricated in TFLN, which exhibits the Pockels effect and enables the modulation of the effective refractive index by applying an external electric field, and single-mode optical waveguides with a center wavelength of 1550 nm. Figure 6 shows the implementation of a MZI in TFLN, detailing key parameters defining the optical transfer function and electrical characteristics, calibrated using Ansys Lumerical, Ansys HFSS and experimentally measured data. All compact models are developed using plain text, so we expect users should be able to easily adjust parameters models for their specific application targets.

The pseudo-code in Algorithms 2 and 3 describe the functionality of the MZI and SOA compact models, respectively, representative of our broadband implementation. The electrodes of the MZI are modeled as an RC network with series resistance (R_{elec}) and capacitance to the substrate (C_{ver}) and adjacent electrodes (C_{hor}). We model the change in refractive index (Δn) as a function of the effective voltage (ΔV_{eff}) using a first-order electro-optical coefficient (eo_{coef}), and we calculate the induced phase change ($\Delta\phi$) across the active length (AL) of the electrodes.

Algorithm 2 2-branch Mach-Zehnder Interferometer

$(\ \mathrm{L_{in}}[0:2*N-1],\ \mathrm{L_{out}}[0:2*N-1],\ \mathrm{V_{elec}}[0:2]\ )$
for $i \in [0,2]$ **do**
  // Creating R-C network to model electrodes
  $\mathrm{I}(V_{elec(i)}, V_{eff(i)}) = \mathrm{V}(V_{elec(i)}, V_{eff(i)})/R_{elec}$
  $\mathrm{I}(V_{eff(i)}, V_{sub}) = C_{ver} * \frac{d[\mathrm{V}(V_{elec}, V_{sub})]}{dt}$
  $\mathrm{I}(V_{eff(i)}, V_{eff(i-1)}) = C_{ver} * \frac{d[\mathrm{V}(V_{elec}, V_{eff(i-1)})]}{dt}$
  $\mathrm{I}(V_{eff(i)}, V_{eff(i+1)}) = C_{hor} * \frac{d[\mathrm{V}(V_{elec}, V_{eff(i+1)})]}{dt}$
end for
$\Delta V_{eff(top)} = \mathrm{LPF}[\mathrm{V}(V_{eff(2)}, V_{eff(1)})]$
$\Delta V_{eff(bot)} = \mathrm{LPF}[\mathrm{V}(V_{eff(1)}, V_{eff(0)})]$
for $i \in [0,2],\ j \in [0,N]$ **do**
  // Using the calculations from 'Algorithm 1'
  $\Delta n_{top(j)} = \Delta V_{eff(top)} * eo_{coef}$
  $\Delta n_{bot(j)} = \Delta V_{eff(bot)} * eo_{coef}$
  $\Delta\phi' = \Delta\phi + 2\pi * \Delta n_{top(j)} * AL/\lambda_j$
  $\Delta\phi'' = \Delta\phi + 2\pi * \Delta n_{bot(j)} * AL/\lambda_j$
  $\begin{matrix}\mathrm{R}\{L_{top(j)}\}\\ I\{L_{top(j)}\}\end{matrix} = \begin{bmatrix}\cos(\Delta\phi') & -\sin(\Delta\phi')\\ \sin(\Delta\phi') & \cos(\Delta\phi')\end{bmatrix} * \begin{matrix}\frac{\mathrm{R}\{L_{in(j)}\}}{\sqrt{2}}\\ \frac{\mathrm{I}\{L_{in(j)}\}}{\sqrt{2}}\end{matrix}$
  $\begin{matrix}\mathrm{R}\{L_{bot(j)}\}\\ I\{L_{bot(j)}\}\end{matrix} = \begin{bmatrix}\cos(\Delta\phi'') & -\sin(\Delta\phi'')\\ \sin(\Delta\phi'') & \cos(\Delta\phi'')\end{bmatrix} * \begin{matrix}\frac{\mathrm{R}\{L_{in(j)}\}}{\sqrt{2}}\\ \frac{\mathrm{I}\{L_{in(j)}\}}{\sqrt{2}}\end{matrix}$
  $L_{out(j)} = (1-10^{-a/20}) * (L_{top(j)} + L_{bot(j)})/\sqrt{2}$
end for

The SOA model supports multiple non-linearities including gain saturation, spectral broadening and Amplified Spontaneous Emission (ASE). Saturation is modeled based on [16] as a function of total optical input power, spectral broadening follows the Gaussian blur methodology and ASE can be modeled as white noise using a Uniform Distribution Function (UDF), or Guassian using a Random Normal Distribution Function (RNDF).

Algorithm 3 Semiconductor Optical Amplifier

$(\ \mathrm{L_{in}}[0:2*N-1],\ \mathrm{L_{out}}[0:2*N-1]\ )$
$P_{total} = \sum_{i=0}^{N} \sqrt{\mathrm{R}\{L_{in(i)}\}^2 + \mathrm{I}\{L_{in(i)}^2\}}$
$Gain' = Gain_{max}/\sqrt{1 + (Gain_{max}^2 - 1) * (P_{in}/P_{sat})}$
for $i \in [0,N]$ **do**
  $P_{in(i)} = \sqrt{\mathrm{R}\{L_{in(i)}\}^2 + \mathrm{I}\{L_{in(i)}^2\}}$
  $P_{ampl} = \sum_{j=i-\frac{\lambda_{spread}}{\lambda_{spacing}}}^{i+\frac{\lambda_{spread}}{\lambda_{spacing}}} P_{in(j)} * NDF_{i,steps}(j)$
  if $White\ Noise$ **then**
    $\Delta L = Noise_{max} * (UDF \in [0,2])$
  else if $Gaussian\ Noise$ **then**
    $\Delta L = Noise_{max} * RNDF_{1,n_{std}}$
  end if
  $\begin{matrix}\mathrm{R}\{L_{out(j)}\}\\ I\{L_{out(j)}\}\end{matrix} = Gain' * \begin{matrix}\mathrm{R}\{L_{in(j)}\}\\ \mathrm{I}\{L_{in(j)}\}\end{matrix} + \Delta L$
end for

C. Heterogeneous Integration, Physical Design & Verification

Many EPICs target high-speed applications, where interconnect parasitics (R, L, C) can bottleneck performance. Simulating these effects is challenging as EICs, PICs, and interconnects are often fabricated at different facilities, each with separate, incapable of interfacing with each other models.

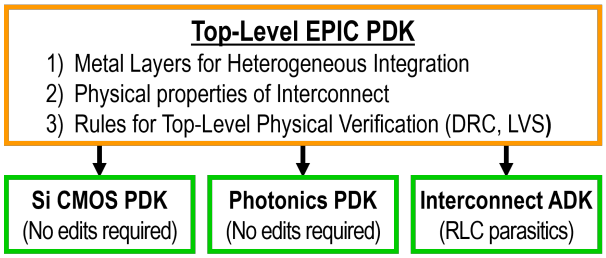

Fig. 8. Top-level EPIC PDK provides interfacecs between electronic and photonic PDKs to enable co-design of electronic and photonic circuits.

To address this, we structure EPIC PDKs *hierarchically*, with a top-level EPIC PDK that *instantiates* multiple electrical PDKs, photonic PDKs, and interconnect models as showcased in Figure 8. For example, our reference EPIC PDK supports the design of a 180 nm silicon CMOS IC (from X-FAB) bonded face-to-face with a TFLN photonic IC. The EPIC PDK is structured as follows:

- Silicon CMOS PDK: *unchanged*; Foundries typically do not adjust their PDKs for heterogeneous integration needs.
- Photonic PDK: *unchanged*; Designed as described in this paper, doesn't require customization depending on the heterogeneous integration strategy.
- Interconnect ADK; Lightweight components for interfacing the electronic and photonic PDK, while verifying the connectivity and constraint satisfaction of the interconnections.

TABLE I
COMPARISON WITH STATE-OF-THE-ART COMMERCIAL TOOLS (*NON-LINEARITIES REFER TO INTER-WAVELENGTH INTERACTIONS)

	This work	Lumerical Interconnect [17]	Lumerical FDTD [18]	Tidy3D [19]
Simulation Type	Compact Model		Finite Elements	
Accuracy	Moderate (Depends on quality of compact models)		High (Detailed field distribution)	
Speed [Fig. 7]	Fast	Fast	Slow	Slow
Experimental Tuning	Yes	Yes	Not Applicable	Not Applicable
Arbitrary Geometries	No	No	Yes	Yes
*Non-linearities**	Yes	No	Yes	Yes
Electronics Co-Simulation	Yes	Yes	No	No
Tool Integration	Full (Built-in Cadence Virtuoso)	Partial (Requires Cadence CurvyCore)	None (Only compact model export)	
User Expertise	Low (IC designers with limited photonics background)		High (Requires extended photonics background)	

III. REFERENCE DESIGNS AND APPLICATIONS

This section includes the design and simulation results of reference designs using our EPIC PDKs for high-speed optical datalinks with WDM (Figure 9), entirely optical unitary matrix multiplication (Figure 10).

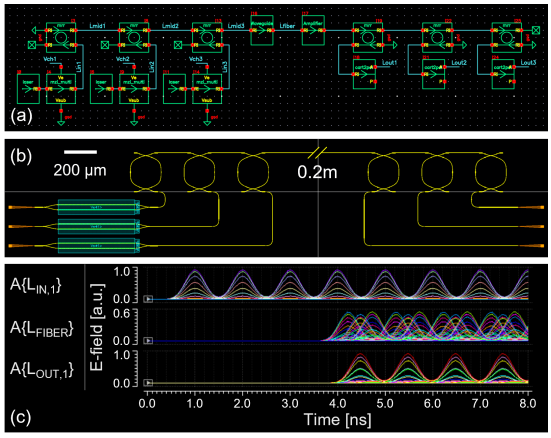

Fig. 9. Example application (A). WDM is a promising technique for high-bandwidth data links, using multiple optical wavelength channels on a single waveguide. It relies on MZMs for transmission and MRRs to filter data at specific frequencies. Despite its advantages, WDM faces challenges from process variations and temperature fluctuations, which can be mitigated through electronic-photonic co-design.

We also evaluate the computational intensity of our reference designs (Table II). We observe that compilation time increases proportionally to the number of wavelengths, while the sharp increase in initial conditions computation time is due to an inherent simulator limitation, related to the node count, as confirmed by the vendor. The transient simulation also scales with wavelengths, but - in contrast to compilation - performs comparably for both linear and non-linear devices because of the compilation step. Also, the computational intensity of electronics remains constant across runs as it is wavelength-independent. Lastly, a key point is leveraging incremental compilation, which allows each design to be compiled only once, while subsequent runs use the already compiled models.

TABLE II
SIMULATION RESOURCES

Design	Duration	λs	CPU Time [s]		
			Compilation	Initial	Transient
A [Fig. 9]	10 ns	10	11.39	1.303	117.4
		100	225.5	1.271	529.8
		1000[1]	1.21k	49.82	4.28k
B [Fig. 10]	5 ns	10	2.913	0.909	32.89
		100	17.20	66.07	540.4
		1000	168.4	14.2k	2.75k

[1]Non-linear SOA model failed to run due to memory restrictions.

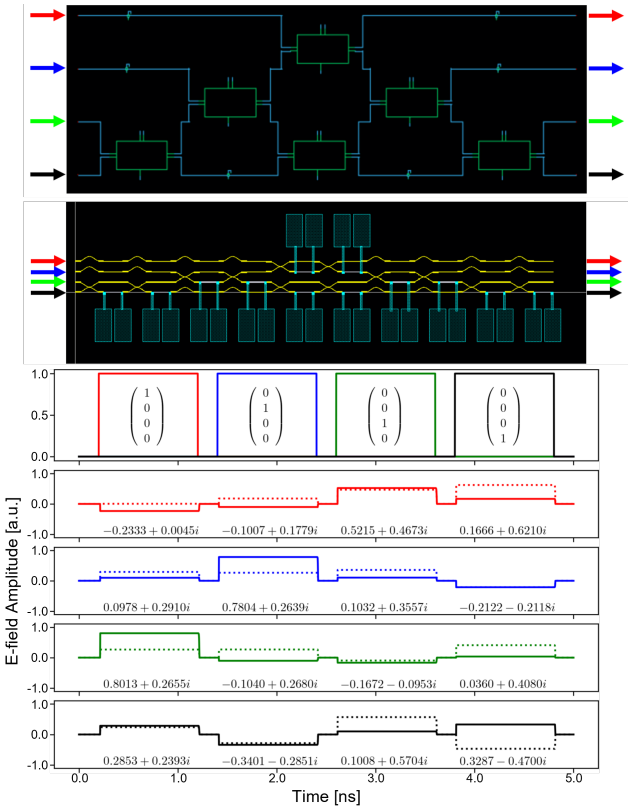

Fig. 10. Example application (B). Research groups have demonstrated small-scale PICs performing high-speed linear operations (e.g., multiplication, addition) [3], but current optical computing systems still rely on electronics for non-linear tasks like activation functions, control flow, and memory. The power and performance costs of converting between optical and electrical domains limit optical computing's benefits. Streamlined electronic-photonic co-design is crucial for optimizing these systems.

IV. CONCLUSION

EPICs enchance performance in communication, computation, and other areas. *Co-designing* electronics and photonics is crucial for maximizing EPIC performance, but challenging, due to the use of of separate CAD tools and PDKs (examples in Table I). This paper provides guidelines for EPIC *PDKs* to address these issues and enable co-design of electronic and photonic circuit components in a *holistic design environment*. In particular, we present techniques for combining *broadband* photonic simulations with electronic simulations using industry-standard CAD tools and design flows. We, also, offer publicly available compact models that implement our techniques, in reference EPIC PDKs and designs, which designers can leverage for their own custom systems.

REFERENCES

[1] Yiwen Shen, Xiang Meng, Qixiang Cheng, Sébastien Rumley, Nathan Abrams, Alexander Gazman, Evgeny Manzhosov, Madeleine Strom Glick, and Keren Bergman. Silicon photonics for extreme scale systems. *Journal of Lightwave Technology*, 37(2):245–259, 2019.

[2] Theonitsa Alexoudi, Nikolaos Terzenidis, Stelios Pitris, Miltiadis Moralis-Pegios, Pavlos Maniotis, Christos Vagionas, Charoula Mitsolidou, George Mourgias-Alexandris, George T Kanellos, Amalia Miliou, et al. Optics in computing: From photonic network-on-chip to chip-to-chip interconnects and disintegrated architectures. *Journal of Lightwave Technology*, 37(2):363–379, 2018.

[3] Farhad Shokraneh, Mohammadreza Sanadgol Nezami, and Odile Liboiron-Ladouceur. Theoretical and experimental analysis of a 4×4 reconfigurable mzi-based linear optical processor. *Journal of Lightwave Technology*, 38(6):1258–1267, 2020.

[4] Jonathan K Doylend and Sanjeev Gupta. An overview of silicon photonics for lidar. *Silicon Photonics XV*, 11285:109–115, 2020.

[5] Tamara Đorđević, Polnop Samutpraphoot, Paloma L Ocola, Hannes Bernien, Brandon Grinkemeyer, Ivana Dimitrova, Vladan Vuletić, and Mikhail D Lukin. Entanglement transport and a nanophotonic interface for atoms in optical tweezers. *Science*, 373(6562):1511–1514, 2021.

[6] Wei Ting Chen, Alexander Y Zhu, and Federico Capasso. Flat optics with dispersion-engineered metasurfaces. *Nature Reviews Materials*, 5(8):604–620, 2020.

[7] Norman Lippok, Jeffrey Holzgrafe, Georgios Kyriazidis, Yongjoo Kim, Xinrui Zhu, Yaowen Hu, Gage Hills, Marko Loncar, Benjamin J Vakoc, and Hana Warner. Integrated time-stepped optical frequency comb laser sources for time-discrete oct. In *Optical Coherence Tomography and Coherence Domain Optical Methods in Biomedicine XXVII*, page PC123670R. SPIE, 2023.

[8] Georgios Kyriazidis, Norman Lippok, John Davis, Xinrui Zhu, Hana Warner, Yaowen Hu, Marko Loncar, Benjamin J Vakoc, and Gage Hills. Time-stepped optical frequency comb laser design leveraging three-dimensional integration of thin-film lithium niobate and silicon cmos. In *Smart Photonic and Optoelectronic Integrated Circuits 2024*, page PC128900M. SPIE, 2024.

[9] Francesco Zanetto, Fabio Toso, Vittorio Grimaldi, Matteo Petrini, Alessandro Perino, Francesco Morichetti, A Melloni, Giorgio Ferrari, and Marco Sampietro. Monolithically integrated cmos electronics in zero-change silicon photonics. In *Emerging Applications in Silicon Photonics III*, volume 12334, page 1233402. SPIE, 2023.

[10] Di Zhu, Linbo Shao, Mengjie Yu, Rebecca Cheng, Boris Desiatov, C. J. Xin, Yaowen Hu, Jeffrey Holzgrafe, Soumya Ghosh, Amirhassan Shams-Ansari, Eric Puma, Neil Sinclair, Christian Reimer, Mian Zhang, and Marko Lončar. Integrated photonics on thin-film lithium niobate. *Adv. Opt. Photon.*, 13(2):242–352, 2021.

[11] Cheng Wang, Xiao Xiong, Nicolas Andrade, Vivek Venkataraman, Xi-Feng Ren, Guang-Can Guo, and Marko Lončar. Second harmonic generation in nano-structured thin-film lithium niobate waveguides. *Optics express*, 25(6):6963–6973, 2017.

[12] Yu Zhang, Anirban Samanta, Kuanping Shang, and SJ Ben Yoo. Scalable 3d silicon photonic electronic integrated circuits and their applications. *IEEE Journal of Selected Topics in Quantum Electronics*, 26(2):1–10, 2020.

[13] Haoyu Wang, Jianshe Ma, Yide Yang, Mali Gong, and Qinheng Wang. A review of system-in-package technologies: Application and reliability of advanced packaging. *Micromachines*, 14(6), 2023.

[14] Yao-Wen Chang. Physical design challenges in modern heterogeneous integration. In *Proceedings of the 2024 International Symposium on Physical Design*, ISPD '24, page 125–134. Association for Computing Machinery, 2024.

[15] Lukas Chrostowski, Hossam Shoman, Mustafa Hammood, Han Yun, Jaspreet Jhoja, Enxiao Luan, Stephen Lin, Ajay Mistry, Donald Witt, Nicolas AF Jaeger, et al. Silicon photonic circuit design using rapid prototyping foundry process design kits. *IEEE Journal of Selected Topics in Quantum Electronics*, 25(5):1–26, 2019.

[16] Farhan Rana. Lecture notes on semiconductor. ECE 5330, Cornell University.

[17] Ansys lumerical interconnect.

[18] Anlsys lumerical fdtd.

[19] Python-driven fdtd software: Flexcompute tidy3d.